Available online at www.sciencedirect.com

ScienceDirect

Ceramics International 40 (2014) 14111–14117

CERAMICS INTERNATIONAL

www.elsevier.com/locate/ceramint

Effect of agglomeration and calcination temperature on the mechanical properties of yttria stabilized zirconia (YSZ)

Ajoy Kumar Pandey[a,*], Koushik Biswas[b]

[a]Department of Metallurgical and Materials Engineering, National Institute of Technology Warangal, Warangal, Andhra Pradesh, India
[b]Department of Metallurgical and Materials Engineering, Indian Institute of Technology, Kharagpur 721302, India

Received 13 May 2014; received in revised form 29 May 2014; accepted 30 May 2014
Available online 7 June 2014

Abstract

Effect of azeotropic distillation after co-precipitation process of powder synthesis on powders morphology and mechanical properties of yttria stabilized zirconia was studied. The formation of hard or soft agglomerates during drying or calcination of co-precipitated powder can easily be prevented through azeotropic distillation. The powder prepared by direct co-precipitation and azeotropic treatment after co-precipitation process was calcined at different temperatures and was characterized through X-ray diffraction, transmission electron microscope and BET surface area measurement. The calcined powders were compacted uniaxially and sintered in two step sintering process. Sintered, polished and thermally etched samples were observed under scanning electron microscope. Vickers hardness and indentation fracture toughness were estimated. It is observed that reasonably higher density with better hardness and fracture toughness can be achieved for azeotroped samples in same sintering condition. Azeotropic treatment increases the surface area almost three times which helps to achieve better sintering. Pin on disc wear tests against alumina disc at 20 N and 50 N loads up to 3000 m distance were carried out. The wear depth and coefficient of friction for both the material were compared.

Keywords: A. Calcination; A. Sintering; D. Y_2O_3; Azeotropic

1. Introduction

Yttria stabilized zirconia (YSZ) has find its wide application as oxygen pump, sensors and catalytic members [1,2] and Ni-YSZ cermet in solid oxide fuel cells [3–6] and thermal barrier coating [7–9]as it shows good oxygen ionic conductivity, high temperature stability and very fine and uniform microstructure. YSZ belongs to the family of transformation toughened ceramics which made YSZ to be tougher. High bending strength, relatively low Young's modulus coupled with fairly high hardness made YSZ very attractive as a biomaterial in load bearing orthopedics and dental application [10–13]. However further improvement of properties as well as phase transformation stability is required which can be achieved through proper tuning of composition as well as microstructure. Microstructure refinement is possible by following proper sintering conditions and also using superior quality (smaller particle, narrow particle size distribution, minimum impurities and agglomerate free) powder for sintering. For synthesizing a better quality powder preferred technique followed by the researchers is wet chemical route. Commonly reported wet chemical process are sol–gel method, co-precipitation, hydrothermal process, spray drying, spray pyrolysis, freeze drying, combustion synthesis, auto ignition, polymer precursor synthesis oxalate precipitation etc. In heterogeneous precipitation techniques, nanosized powder can be easily synthesized but they get agglomerated during drying or calcination. An agglomerated powder (it may have very fine particle size) does not always show good sinterability [14]. Final powder property largely depends upon the fraction of agglomerate present in the powder.

A clatter of primary particles held together by surface forces, by liquid, or by a solid bridge is called agglomerate. There are two kinds of agglomerates, soft (particles are held together by

*Corresponding author.
E-mail address: ajoy100@gmail.com (A.K. Pandey).

http://dx.doi.org/10.1016/j.ceramint.2014.05.144
0272-8842/

weak van der Waals forces) and hard (particles are chemically bonded together by strong bridges) [15]. The soft agglomerates formed during synthesis becomes more stronger during calcination [16,17] and during sintering they produces microstructural in-homogeneities [18]. The hard agglomerates often hinder densification and develop flaws inside the material during sintering [19]. Soft agglomerates does not affect much as the hard one do. The degree of hardness of agglomerates is determined by the ability of water molecules and/or hydroxyl groups incorporated in the co-ordinated structure to form strong oxygen bridges between adjacent particles [19].

As proposed by different researchers, the excess water molecules of colloidal solution interact with terminal (free) hydroxyl group through hydrogen bonding and they act as "bridges" to draw neighboring particles together. When powders are been dried, the excess water comes out drawing the neighboring particles closer. Now the nonbridging hydroxyl groups on adjacent particles try to interact with themselves and if they are sufficiently close enough, they conducts the following condensation reaction, forming strong chemical bond between neighboring particles [19–21].

$$Zr–OH + HO–Zr \rightarrow Zr–O–Zr + H_2O \quad (1)$$

Formation of hard agglomerates can be avoided to a great extent by dehydrating the synthesized powder through azeotropic distillation process forming water-organic solvent binary azeotrope. The organic solvent (n-butanol, n-propanol, etc.) acts as a "water carrier" in this process. During azeotropic distillation process, the excess water molecules in the colloid are removed and the hydroxyl groups (OH) on the surface of the particles are replaced by butoxyl groups (OC_4H_9); in case of n-butanol taken as an organic solvent. This replacement eliminates the possibility of formation of hydrogen bond as well as strong chemical bond (hard agglomerates) at the latter stage. In this study, the effects of agglomerates on mechanical and tribological properties were studied. Agglomerated and agglomerate free powders were synthesized through direct co-precipitation technique and azeotropic distillation process.

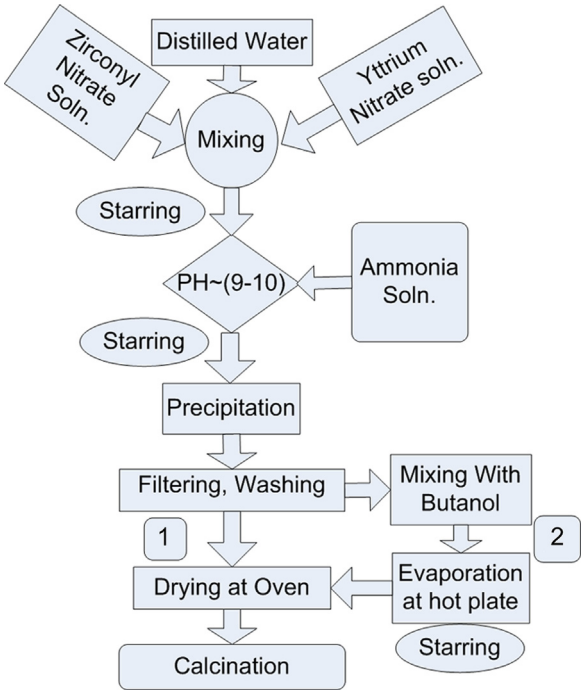

Fig. 1. Schematic representation of powder preparation process.

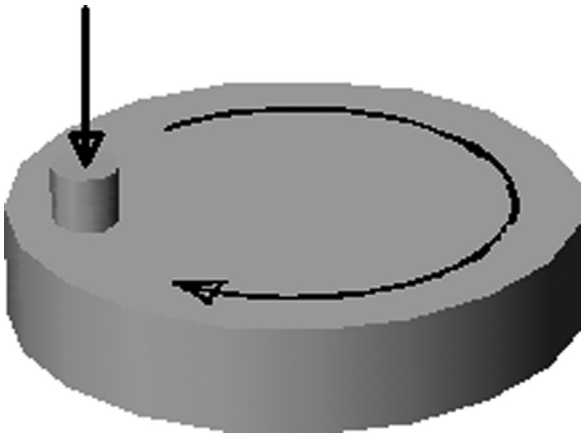

Fig. 2. Schematic representation of pin on disc wear configuration.

2. Materials and methods

2.1. Processing

8 mol% Yttria stabilized zirconia (YSZ) powder were synthesized using wet chemical method from their respective nitrate salts; zirconyl nitrate (Loba chemie, India, $>99.5\%$ pure) and yttrium nitrate (Strem chemicals, USA, 99.9% pure). As shown in Fig. 1, the proportionate quantities of precursor salts were dissolved in distilled water and then drop wise ammonia solution was added to the dissolved salts. The solution was vigorously starred by a magnetic starrer during ammonia addition. Precipitation was completed in the pH range of 9–10. One hour ageing time at this pH range was provided for complete precipitation. The precipitate was then filtered and washed several times with distilled water. Vacuum filter was used for maximum probable water removal from the washed gel. The filtrate was then divided into two parts. The first part was directly dried overnight at 120 °C (route one) and the rest was mixed with n-butanol under vigorous mechanical agitation as they are not mutually wet able at room temperature (only about 10 wt% of water is miscible in n-butanol at room temperature). The mixture was then dried in a hot plate (route two). While drying the solution was continuously stirred with magnetic stirrer. Finally the precipitate was transferred to an oven and dried overnight at 120 °C.

Both the powders obtained from route one and two, were calcined at 600, 800, 1000 and 1200 °C for 2 h in order to achieve variation in particle size. The calcined powders were then uniaxially pressed to pallets of $\Phi = 10$ mm and $t = 3$ mm using 600 MPa. The compacted pallets were sintered in two step sintering process (1500 °C for 30 min and 1300 °C for 14 h) at average heating rate @ 5 °C min^{-1}) in a resistance heated tube furnace (Bysakh and Co, India).

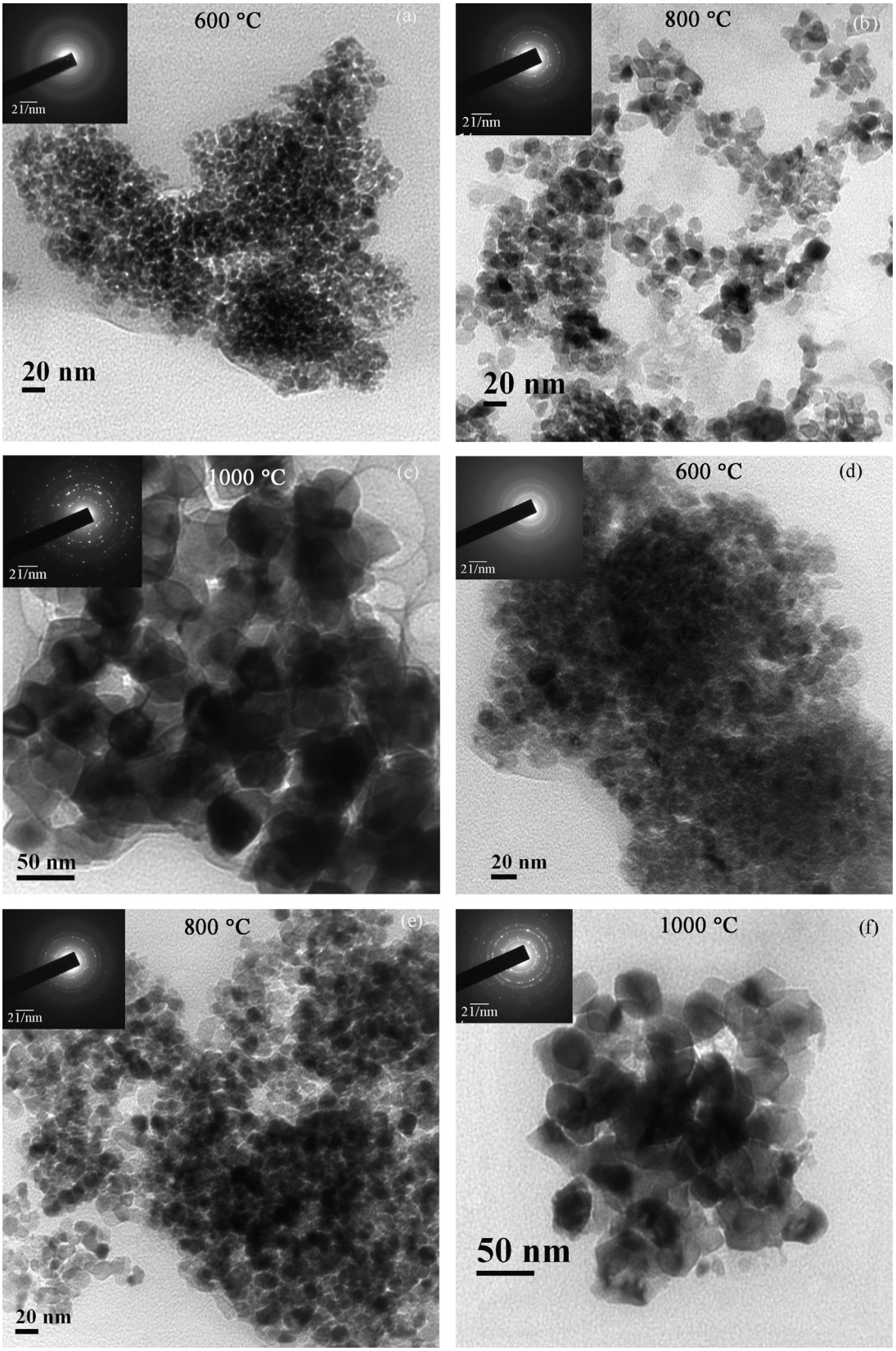

Fig. 3. TEM images of powders calcined at different temperatures. (a)–(c) Butanol treated powders after co-precipitation. (d)–(f) Direct co-precipitated powders. Temperature mentioned in figure indicates calcination temperature.

2.2. Characterizations

The specific surface area of calcined powders was estimated through BET method using NOVA® Surface Area Analyzer (Quanta chrome, USA). Particle size was calculated from the measured specific surface area using the following equation:

$$D_{BET} = \frac{6 \times 10^3}{\rho S_{BET}}$$

where D_{BET} is the average particle size (nm), S_{BET} is the specific surface area ($m^2\ g^{-1}$), ρ is the theoretical density of YSZ expressed in $g\ cm^{-3}$.

The particle size and distribution were estimated by observing the powders under a transmission electron microscope (TEM) (JEM 2100, Geol, Japan). The samples for TEM were prepared by dispersing the calcined powders in carbon coated copper grids. The powders were ultrasonically dispersed in the presence of a dispersant (2–3 wt% ammonium polyacrilate [22]) in distilled water during sample preparation of TEM. X-ray diffraction (XRD) patterns were obtained with $Cu_{K\alpha}$ radiation ($\lambda = 1.5406$ Å) operated at 40 kV, 25 mA, taking step size of 0.03, time per step = 1 min, using High Resolution X-ray diffractometer (PANalytical, X′Pert PRO, Phillips, The Netherlands). The patterns were analyzed by Rietveld method using the software X′Pert High score Plus (PANalytical B.V., Almelo, The Netherlands) to know the phase present and their relative quantity. Sintered, polished and thermally etched (1200 °C for 1 h) specimens were observed under scanning electron microscope (SEM) (SUPRA − 40, Carl Zeiss, Germany). The sintered densities of the samples were measured by Archimedes' principle. Vickers indentation hardness was measured on bulk sintered specimens with 200 N load with 15 s dual time using LECO Hardness Tester (LV 700, LECO Corporation, USA). Indentation fracture toughness was measured according to Anstis et al. [23]. Comparative pin on disc wear were carried out on both kind of samples ($R_a \sim 0.03$ μm) applying 50 N load at 150 RPM for 2 h using TE97 friction and wear demonstrator (Phoenix Tribology Ltd., England). The schematic of sample position, disc rotation and direction of load implementation during wear are shown in Fig. 2. An alumina disc was used as a counter body. Wear depth and frictional force (to estimate coefficient of friction) were continuously recorded through two different sensors during experiment.

3. Results and discussions:

Fig. 3 shows the TEM images of normal co-precipitated and butanol treated powders which were calcined at different temperatures. It is clear from Fig. 3, that nanosized powder with varying particle size (5–45 nm) with calcination temperature can be achieved. As shown in TEM images, the two kind of powder does not show much difference in respect to particle size. During TEM sample preparation the mechanical agitation and ultrasonic vibration broke the agglomerates (Zr–O–Zr bond) and the use of dispersant keep them separate during drying of TEM samples, resulting the same microstructure for both kind of powders. The azeotropic modification does not

Table 1
Comparative surface area, particle size and mechanical properties of route 1 and 2.

Calcination temperature (°C)	BET surface area (m^2/g)		Particle size (nm)				Hardness (VHN)		Fracture toughness (MPa$\sqrt{m}$)	
			BET		TEM					
	B[a]	WB	B	WB	B	WB	B	WB	B	WB
600	145	56	7	18	6	–	1364 ± 11	1088 ± 10	16.25 ± 2.60	10.69 ± 0.81
800	65	38	16	27	14	14	1240 ± 08	824 ± 10	8.11 ± 2.28	8.99 ± 0.99
1000	35	10	29	102	35	35	1161 ± 12	717 ± 05	7.72 ± 0.28	6.47 ± 0.64

[a]B = butanol treated, WB = without butanol.

have any effect on the particle size; it only prevents the formation of hard agglomeration.

As expected, the BET surface area of butanol treated powders is significantly higher than as synthesized powders. It has increased around three times in case of 600 °C calcined powders (Table 1). As expected, the surface area has decreased with the increase of calcination temperature, for both the powders due to increased particle size during higher temperature calcination. A comparative particle size obtained through TEM and BET surface area analysis is shown in Table 1. As discussed earlier, azeotropic modification prevents the formation of hard agglomerates during drying or calcination resulting enhanced surface area value.

Significant increase (about 25%) in hardness value (increased up to 1365HV20) as well as toughness is achieved in butanol treated samples (Table 1). This is due to better sinterablity of agglomerate free powders. Similar trends are also found by other researchers through mixing high pure powders in n-propanol and drying over rotating evaporator [24] and using glycine–nitrate process and ball milling the synthesized powder [25]. In all the cases such excellent property is due to the secondary operation (n-propanol treatment or milling) after powder synthesis which breaks the agglomerates.

The effect of agglomerates on green density as well as sintered density is shown in Fig. 4. As expected the green density for agglomerate free powder is lower than that of agglomerated powder at same compaction pressure (600 MPa). Finer particle poses larger surface area which exhibits higher inter-particle friction during compaction. Enhanced frictional resistance reduces the effectively available pressure for compaction which results poor green density. Particle size increases with the increase of calcination temperature. Hence we observe the increase in green density with the increase of calcination temperature irrespective to the synthesis route. As expected the sintered density of agglomerate free powder is higher than that of agglomerated one (Fig. 4). The weight loss during calcination is also plotted in Fig. 4. The powders were predried at 150 °C to ensure removal of external moisture

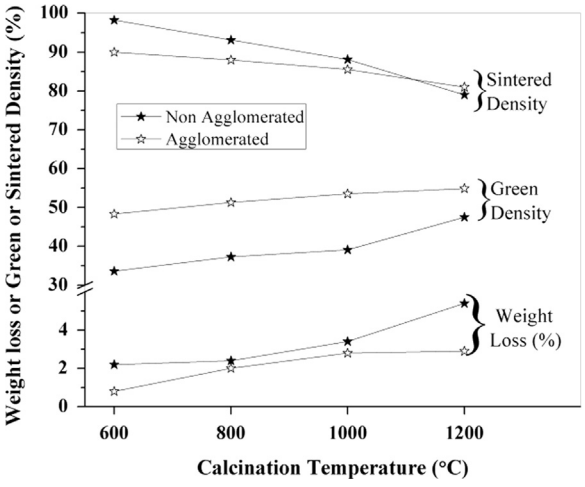

Fig. 4. Variation of densities and weight loss during calcination with calcination temperature.

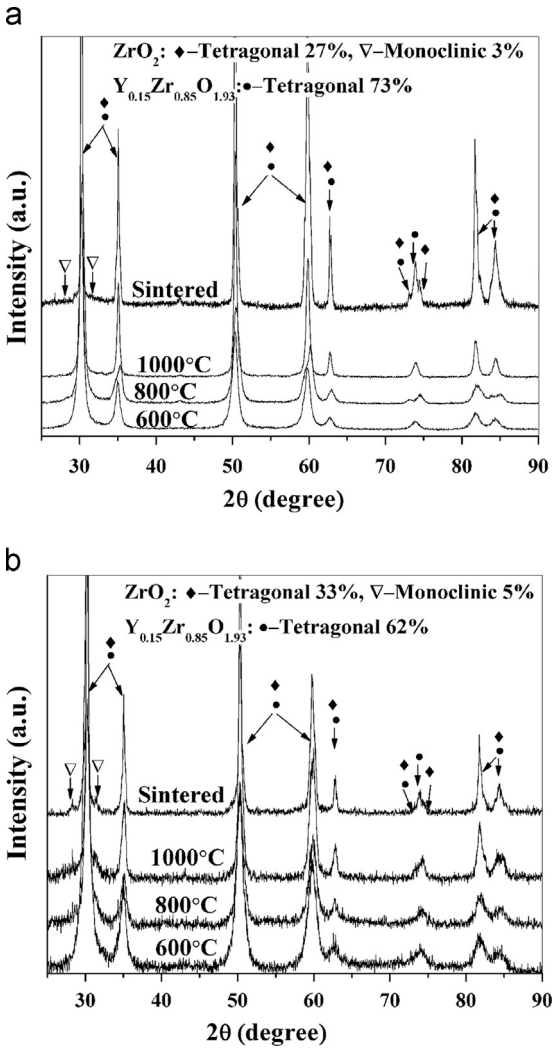

Fig. 5. XRD patterns representing the phase content of (a) butanol treated samples and (b) direct co-precipitated samples.

before measuring the weight before calcination. It is seen that butanol treated powders exhibits a little weight loss during calcination. This may be due to the higher molecular weight of butoxyl groups (OC_4H_9) than hydroxyl groups (OH). During azeotropic modification some hydroxyl groups were replaced by butoxyl groups and those butoxyl groups were removed during calcination. Loss of those butoxyl groups increases with increase in calcination temperature, resulting increased weight loss with the increase of calcination temperature.

Although the starting particle size of both the powders were same (Fig. 3) the agglomerates makes the difference. An agglomerated powder causes heterogeneous packing in the green body. As a result, during sintering, different part shrinks at different rate (differential sintering) leading localized densification. This results larger pore and crack like voids (significant fraction of porosity) [26]. The densification rate is roughly similar to that for a course grained body with a particle size equivalent to that of the agglomerates [15]. The densification rate is inversely proportional to the forth power of particle

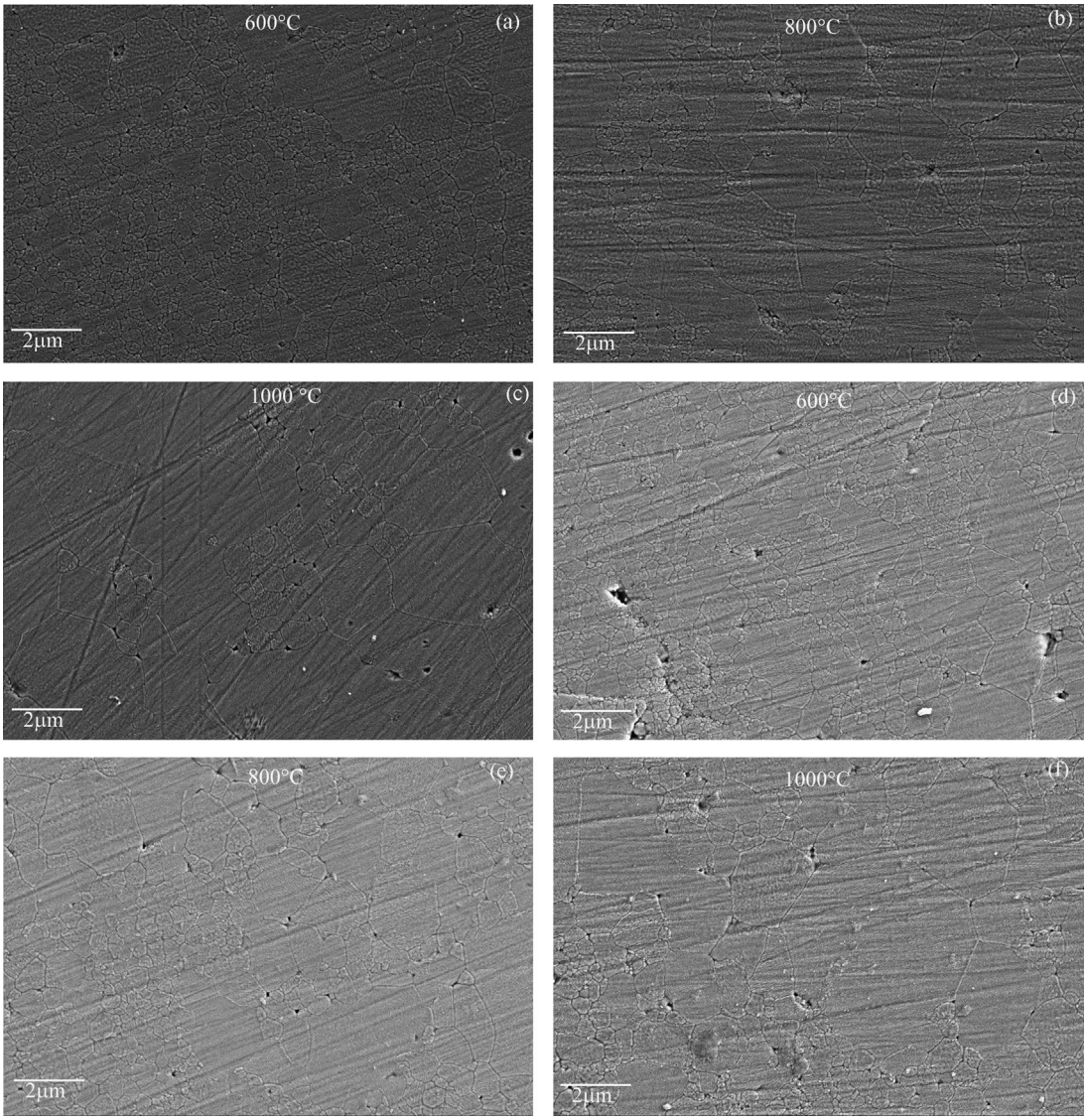

Fig. 6. SEM images of sintered, polished and thermally etched samples. (a)–(c) Butanol treated samples and (d)–(f) direct co-precipitated samples.

size hence fine and narrow size distributed powder always shows enhanced sinterability.

Fig. 5 shows comparative XRD patterns of both kind of powders. Rietveld refinement of sintered specimens shows the presence of tetragonal (ZrO_2 and $Y_{0.15}Zr_{0.85}O_{1.93}$) and little amount of monoclinic (2% in case of butanol treated and 5% in case of nontreated samples) phase. Hence it is clear from Fig. 5 that azeotropic treatment does not have much effect on the phase content of calcined powders as well as sintered objects.

Microstructure of sintered specimens (Fig. 6) clearly shows abnormal grain growth with significantly coarse grain size in case of agglomerated powders. On the other hand submicron sized grain (~0.5 μm) can be achieved with agglomerate free powders at the same sintering schedule. The abnormality of grain and grain size increases with the increase of calcination temperature of both the set of powder but the rate is higher in case of agglomerated powders.

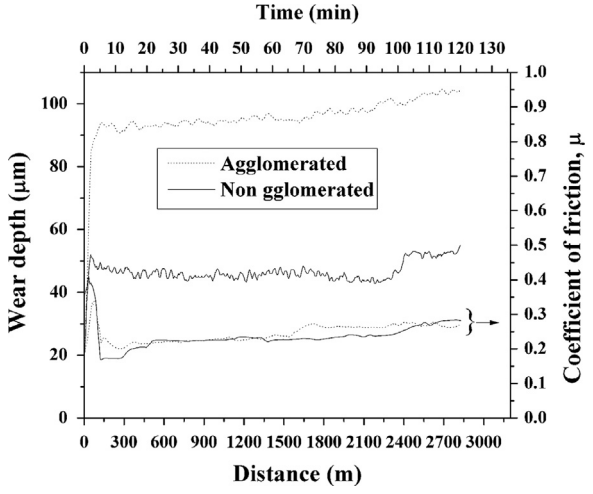

Fig. 7. Wear depth and coefficient of friction against alumina disc achieved at 50 N load in pin on disc configuration.

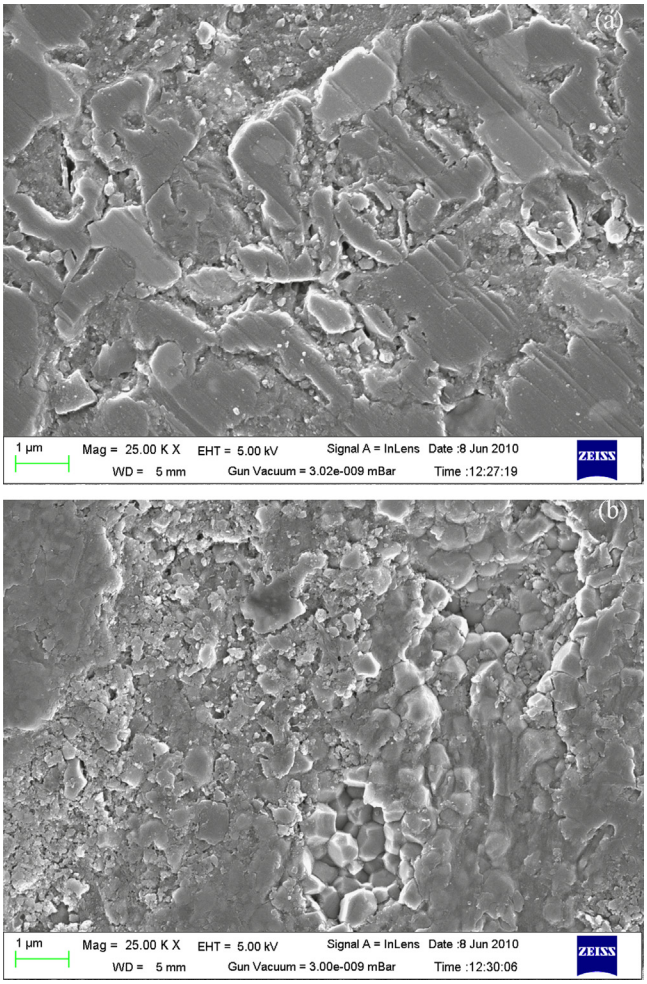

Fig. 8. SEM images of worn out surface (a) direct co-precipitated samples and (b) butanol treated samples.

Fig. 7 shows the comparative profile of wear depth and coefficient of friction of both kinds of samples. The two kinds of samples show similar value for coefficient of friction but butanol treated sample shows less wear depth at the same load (50 N). The final wear depth for as sintered sample is almost twice than that of butanol treated samples. SEM images of worn out surface (Fig. 8) shows clear evidence of plowing, delimitation and grain pullout in the surface which is more prominent in as sintered sample.

4. Conclusions

Azeotropic treatment with organic solvents can prevent the formation of agglomerates during drying or calcination of co-precipitated powders. It increases BET surface area significantly without affecting the relative phase content. Almost 98% dense and submicron sized grain structured specimen with hardness value up to 1365HV20 and toughness value up to 16 MPa$\sqrt{m}$ can be achieved.

References

[1] A. Lashtabeg, J. Drennan, R. Knibbe, J.L. Bradley, G.Q. Lu, Synthesis and characterisation of macroporous Yttria Stabilised Zirconia (YSZ) using polystyrene spheres as templates, Microporous Mesoporous Mater. 117 (2009) 395–401.
[2] Z. Wang, R. Hui, N. Bogdanovic, Z. Tang, S. Yick, Y. Xie, I. Yaroslavski, A. Burgess, R. Maric, D. Ghosh, Plasma spray synthesis of ultra-fine YSZ powder, J. Power Sources 170 (2007) 145–149.
[3] J. Liu, S. Barnett, Thin yttrium-stabilized zirconia electrolyte solid oxide fuel cells by centrifugal casting, J. Am. Ceram. Soc. 85 (2002) 3096–3098.
[4] Y. Du, N. Sammes, Fabrication and properties of anode-supported tubular solid oxide fuel cells, J. Power Sources 136 (2004) 66–71.
[5] J. Kim, R. Song, K. Song, S. Hyun, D. Shin, H. Yokokawa, Fabrication and characteristics of anode supported flat-tube solid oxide fuel cell, J. Power Sources 122 (2003) 138–143.
[6] S. Ramanathan, K. Krishnakumar, P. De, S. Banerjee, Powder dispersion and tape casting of YSZ–NiO composite, J. Mater. Sci. 39 (2004) 3339–3344.
[7] R. Benner, A. Nagelberg, Characterisation of ZrO_2–Y_2O thermal barrier coatings by Raman spectroscopy, Thin Solid Films 84 (1981) 89–94.
[8] C. Funke, J.C. Mailand, B. Siebert, R. Vaβen, D. Stöver, Characterization of ZrO_2–7 wt% Y_2O_3 thermal barrier coatings with different porosities and FEM analysis of stress redistribution during thermal cycling of TBCs, Surf. Coat. Technol. 94–95 (1997) 106–111.
[9] V. Lughi, V. Tolpygo, D. Clarke, Microstructural aspects of the sintering of thermal barrier coatings, Mater. Sci. Eng. A 368 (2004) 212–221.
[10] C. Piconi, G. Maccauro, F. Muratori, E. Prever, Alumina and zirconia ceramics in joint replacements, J. Appl. Biomater. Biomech. 1 (2003) 19–32.
[11] S. Pilathadka, D. Vahalová, T. Vosáhlo, The zirconia: a new dental ceramic material. An overview, Prague Med Rep 108 (2007) 5–12.
[12] C. Piconi, W. Burger, H. Richter, A. Cittadini, G. Maccauro, V. Covacci, N. Bruzzese, G. Ricci, E. Marmo, Y-TZP ceramics for artificial joint replacements, Biomaterials 19 (1998) 1489–1494.
[13] P. Christel, A. Meunier, M. Heller, J. Torre, C. Peille, Mechanical properties and short-term in-vivo evaluation of yttrium-oxide-partially-stabilized zirconia, J. Biomed. Mater. Res. 23 (1) (1989) 45–61.
[14] S.-J. L Kang, Sintering, Densification, Grain Growth, and Microstructure, Elsevier Butterworth-Heinemann, Burlington, 2005.
[15] M. Rahaman, Ceramic Processing and Sintering, second ed., CRC Press, Taylor & Francis Group, New York, USA, 2003.
[16] W. Rhodes, Agglomerate and particle size effects on sintering yttria-stabilized zirconia, J. Am. Ceram. Soc. 64 (1) (1981) 19–22.
[17] M.V.D. Graaf, K. Keizer, A. Buggraff, Influence of agglomerate structures in ultra-fine substituted zirconia powders on compaction and sintering behaviour, Sci. Ceram. 10 (1979) 83–92.
[18] N. Ghoneim, S. Hanna, Sintering and microstructure of ultrafine yttriazirconia compacts, J. Mater. Sci. 25 (1990) 5192–5198.
[19] H. Qiu, L. Gao, C. Feng, J. Guo, D. Yan, Preparation and characterization of nanoscale Y-TZP powder by heterogeneous azeotropic distillation, J. Mater. Sci. 30 (1995) 5508–5513.
[20] S. Zha, Q. Fu, Y. Lang, C. Xia, G. Meng, Novel azeotropic distillation process for synthesizing nanoscale powders of yttria doped ceria electrolyte, Mater. Lett. 47 (2001) 351–355.
[21] H. Qiu, L. Gao, H. Qiao, J. Guo, D. Yan, Nanocrystalline zirconia powder processing through innovative wet-chemical methods, Nanostruct. Mater. 6 (1995) 373–376.
[22] M. Hashiba, H. Okamoto, Y. Nurishi, K. Hiramatsu, Dispersion of ZrO_2 particles in aqueous suspensions by ammonium polyacrylate, J. Mater. Sci. 24 (1989) 873–876.
[23] G. Anstis, P. Chantikul, B. Lawn, D. Marshall, A critical evaluation of indentation techniques for measuring fracture toughness: I, direct crack measurements, J. Am. Ceram. Soc. 64 (4) (1981) 533–538.
[24] N. Gupta, P. Mallik, B. Basu, Y-TZP ceramics with optimized toughness: new results, J. Alloys Compd. 379 (2004) 228–232.
[25] M. Mazaheri, A. Zahedi, M. Hejazi, Processing of nanocrystalline 8 mol % yttria-stabilized zirconia by conventional, microwave-assisted and two-step sintering, Mater. Sci. Eng. A 492 (2008) 261–267.
[26] M. Readey, R. Lee, J. Halloran, A. Heuer, Processing and sintering of ultrafine MgO–ZrO_2 and (MgO, Y_2O_3)–ZrO_2 powders, J. Am. Ceram. Soc. 73 (6) (1990) 1499–1503.